

# A RELATION BETWEEN MASS AND RADIUS FOR 60 EXOPLANETS SMALLER THAN 4 EARTH RADII

LAUREN M. WEISS<sup>1,†</sup> & GEOFFREY W. MARCY<sup>1</sup>

<sup>1</sup>B-20 Hearst Field Annex, Astronomy Department, University of California, Berkeley, CA 94720

*Draft version November 14, 2013*

## ABSTRACT

We study the masses and radii of 60 exoplanets smaller than  $4R_{\oplus}$ . We find and adopt a power-law relation  $M_P/M_{\oplus} = 2.6 (R_P/R_{\oplus})^{1.1}$ . The RMS of planet masses to this fit is  $3.8 M_{\oplus}$ , and our best fit has reduced  $\chi^2 = 2.2$ , indicating a large diversity in planet compositions below  $4R_{\oplus}$ . The exoplanets in our sample have orbital periods between 0 and 100 days. Wu & Lithwick (2013) find  $M_P = 3R_P$  in 22 pairs of planet candidates exhibiting transit timing variations, of which only 10 planets overlap with our sample. The linear mass-radius relation translates to a decrease in planet density with increasing radius. Fitting density vs. radius with a polynomial, we find  $\rho = 10.3 - 5.0R_P + 0.7R_P^2$ . Exoplanets have densities comparable to that of Earth at about  $1.5R_{\oplus}$ ; exoplanets smaller than  $1.5R_{\oplus}$  are typically denser than Earth, indicating likely rocky compositions, whereas exoplanets larger than  $1.5R_{\oplus}$  are typically less dense than Earth, indicating a significant fraction of H/He or water in their compositions. Including the Solar system, we find a tentative mass-radius relationship for terrestrial planets:  $M_P/M_{\oplus} = 1.1 (R_P/R_{\oplus})^{3.4}$ .

## 1. INTRODUCTION

The Kepler Mission has found an abundance of planets with  $R < 4R_{\oplus}$  (Batalha et al. 2013). Although there are no planets between the size of Earth and Neptune in the solar system, occurrence calculations that de-bias the orbital geometry and completeness of the Kepler survey find that planets between the size of Earth and Neptune are common in our galaxy, occurring around at least 24% of stars (Petigura et al. 2013). However, in many systems, it is difficult to measure the masses of such small planets because the gravitational acceleration these planets induce on their host stars or neighboring planets is too small to detect with current telescopes and instruments. Obtaining measurements of the masses of these planets and characterizing their compositions is vital to understanding the formation and evolution of these planets.

Many scientists have explored the relation between planet mass and radius in the Solar system and beyond as a means for understanding exoplanet compositions (Lissauer et al. 2011; Enoch et al. 2012; Kane & Gelino 2012; Seager et al. 2007; Weiss et al. 2013). Figure 1 shows the masses and radii of 147 exoplanets from which such relations can be derived. Below  $4R_{\oplus}$ , the large apparent scatter in planet mass impedes accurate predictions of planet mass. At  $2R_{\oplus}$ , planets are observed to span a decade in density, from less dense than water to densities suggesting a solid iron composition. This scatter could result from a gross underestimate of errors, but is more likely the result of compositional variety among low-mass exoplanets.

In this paper, we investigate mass-radius relationships for planets smaller than 4 Earth radii and explore a tentative mass-radius relationship for terrestrial planets smaller than  $1.5 R_{\oplus}$ . We also investigate how system properties contribute to the scatter in the mass-radius re-

lation by examining how these properties correlate with the residuals of the mass-radius relation.

## 2. SELECTING EXOPLANETS WITH MEASURED MASS AND RADIUS

We choose planets with masses that are (1) well-determined by radial velocities (RVs), (2) well-determined by transit timing variations (TTVs), and (3) marginally determined by RVs. Marcy et al. (2013) measure the masses of 42 small, transiting planets. The planets were selected for their small size, and not based on predictions of their masses. Therefore, these 42 new transiting planets offer an unbiased survey of the masses of small planets. In this paper, we examine the relation between exoplanet mass and radius for the 40 exoplanets smaller than  $4R_{\oplus}$  from Marcy et al. (2013), plus 19 exoplanets smaller than  $4R_{\oplus}$  from the literature, for a total of 60 exoplanets. Histograms of the distributions of planet radius, mass, and density are shown in Figure 2, and the individual measurements of planet mass and radius are shown in Figure 3 and listed in Table 1.

### 2.1. Including Mass Non-Detections for Statistical Soundness

For small exoplanets, uncertainties in the mass measurements for individual planets can be of order the planet mass. Although one might advocate for only studying planets with well-determined ( $> 3\sigma$ ) masses, imposing a significance criterion will bias the sample toward more massive planets at a given radius. This is especially true for small planets, for which the planet-induced RV signal ( $\sim 1\text{ m s}^{-1}$ ) can be small compared to the noise from stellar activity ( $\sim 5\text{ m s}^{-1}$ ). We must include the mass non-detections in order to consider a statistically unbiased sample of planet masses.

Although there is no physical reason that the stellar activity should phase with the orbit of a planet, random statistical fluctuations in tens of RVs can produce RVs that are high when they should be high, and low when

<sup>†</sup> Supported by the NSF Graduate Student Fellowship, Grant DGE 1106400.

**Table 1**  
Exoplanets with Mass Upper Limits and  $R_P < 4R_\oplus$

Name	Per (d)	Mass <sup>a</sup> ( $M_\oplus$ )	Radius ( $R_\oplus$ )	Flux ( $F_\oplus$ )	First Ref.	Mass Ref.
55 Cnc e	0.737	8.38±0.39	2.21±0.15	2439.690	McArthur et al. (2004)	Endl et al. (2012)
CoRoT-7 b	0.854	7.42±1.21	1.58±0.1	1779.433	Queloz et al. (2009); Léger et al. (2009)	Hatzes et al. (2011)
GJ 1214 b	1.580	6.45±0.91	2.65±0.09	16.631	Charbonneau et al. (2009)	Carter et al. (2011)
HD 97658 b	9.491	7.87±0.73	2.34±0.16	48.106	Howard et al. (2011)	Dragomir et al. (2013)
Kepler-10 b	0.837	4.54±1.25	1.42±0.03	3572.048	Batalha et al. (2011)	Batalha et al. (2011)
<sup>b</sup> Kepler-11 b	10.304	1.90±1.20	1.80±0.04	126.512	Lissauer et al. (2011)	Lissauer et al. (2013)
<sup>b</sup> Kepler-11 c	13.024	2.90±2.20	2.87±0.06	91.443	Lissauer et al. (2011)	Lissauer et al. (2013)
<sup>b</sup> Kepler-11 d	22.684	7.30±1.10	3.12±0.07	43.563	Lissauer et al. (2011)	Lissauer et al. (2013)
<sup>b</sup> Kepler-11 f	46.689	2.00±0.80	2.49±0.06	16.747	Lissauer et al. (2011)	Lissauer et al. (2013)
Kepler-18 b	3.505	6.90±3.48	2.00±0.10	462.244	Borucki et al. (2011)	Cochran et al. (2011)
Kepler-20 b	3.696	8.47±2.12	1.91±0.16	346.711	Borucki et al. (2011)	Gautier et al. (2012)
Kepler-20 c	10.854	15.73±3.31	3.07±0.25	82.445	Borucki et al. (2011)	Gautier et al. (2012)
Kepler-20 d	77.612	7.53±7.22	2.75±0.23	5.985	Borucki et al. (2011)	Gautier et al. (2012)
<sup>b</sup> Kepler-30 b	29.334	11.3±1.4	3.90 ±0.20	21.496	Borucki et al. (2011)	Sanchis-Ojeda et al. (2012)
<sup>b</sup> Kepler-36 b	13.840	4.46±0.30	1.48±0.03	217.365	Borucki et al. (2011)	Carter et al. (2012)
<sup>b</sup> Kepler-36 c	16.239	8.10±0.53	3.68±0.05	175.646	Carter et al. (2012)	Carter et al. (2012)
Kepler-68 b	5.399	8.30±2.30	2.31±0.03	409.092	Borucki et al. (2011)	Gilliland et al. (2013)
Kepler-68 c	9.605	4.38±2.80	0.95±0.04	189.764	Batalha et al. (2013)	Gilliland et al. (2013)
Kepler-78 b	0.354	1.78±0.30	1.20±0.09	3093.388	Sanchis-Ojeda et al. (2013)	Howard et al. (2013)
KOI-41.01	12.816	0.85±4.00	2.20±0.05	213.371	Borucki et al. (2011)	Marcy et al. (2013)
KOI-41.02	6.887	7.34±3.20	1.32±0.04	472.831	Borucki et al. (2011)	Marcy et al. (2013)
KOI-41.03	35.333	-4.36±4.10	1.61±0.05	55.812	Borucki et al. (2011)	Marcy et al. (2013)
KOI-69.01	4.727	2.59±2.00	1.50±0.03	220.120	Borucki et al. (2011)	Marcy et al. (2013)
KOI-82.01	16.146	8.93±2.00	2.22±0.07	17.278	Borucki et al. (2011)	Marcy et al. (2013)
KOI-82.02	10.312	3.80±1.80	1.18±0.04	31.184	Borucki et al. (2011)	Marcy et al. (2013)
KOI-82.03	27.454	0.62±3.30	0.88±0.03	8.250	Borucki et al. (2011)	Marcy et al. (2013)
KOI-82.04	7.071	-1.58±2.00	0.58±0.02	51.315	Borucki et al. (2011)	Marcy et al. (2013)
KOI-82.05	5.287	0.41±1.60	0.47±0.02	78.407	Borucki et al. (2011)	Marcy et al. (2013)
KOI-94 b	3.743	10.50±4.60	1.71±0.16	1155.374	Batalha et al. (2013)	Weiss et al. (2013)
KOI-104.01	2.508	10.84±1.40	3.51±0.15	214.674	Borucki et al. (2011)	Marcy et al. (2013)
KOI-108.01	15.965	14.11±4.70	3.37±0.09	124.197	Borucki et al. (2011)	Marcy et al. (2013)
KOI-116.01	13.571	10.44±3.20	2.50±0.32	84.462	Borucki et al. (2011)	Marcy et al. (2013)
KOI-116.02	43.844	11.17±5.80	2.56±0.33	15.645	Borucki et al. (2011)	Marcy et al. (2013)
KOI-116.03	6.165	0.15±2.80	0.82±0.11	239.077	Borucki et al. (2011)	Marcy et al. (2013)
KOI-116.04	23.980	-6.39±7.00	0.95±0.13	43.146	Borucki et al. (2011)	Marcy et al. (2013)
KOI-122.01	11.523	13.00±2.90	3.42±0.09	182.708	Borucki et al. (2011)	Marcy et al. (2013)
KOI-123.01	6.482	1.30±5.40	2.37±0.07	444.879	Borucki et al. (2011)	Marcy et al. (2013)
KOI-123.02	21.223	2.22±7.80	2.52±0.07	94.934	Borucki et al. (2011)	Marcy et al. (2013)
KOI-148.01	4.778	3.94±2.10	1.88±0.10	168.932	Borucki et al. (2011)	Marcy et al. (2013)
KOI-148.02	9.674	14.61±2.30	2.71±0.14	225.109	Borucki et al. (2011)	Marcy et al. (2013)
KOI-148.03	42.896	7.93±4.60	2.04±0.11	13.545	Borucki et al. (2011)	Marcy et al. (2013)
KOI-153.01	8.925	-4.60±6.20	2.19±0.06	50.981	Borucki et al. (2011)	Marcy et al. (2013)
KOI-153.02	4.754	7.10±3.30	1.82±0.05	63.986	Borucki et al. (2011)	Marcy et al. (2013)
KOI-244.02	6.239	9.60±4.20	2.71±0.05	667.269	Borucki et al. (2011)	Marcy et al. (2013)
KOI-245.01	39.792	1.87±9.08	1.94±0.06	7.710	Borucki et al. (2011)	Marcy et al. (2013)
KOI-245.02	21.302	3.35±4.00	0.75±0.03	16.291	Borucki et al. (2011)	Marcy et al. (2013)
KOI-245.03	13.367	2.78±3.70	0.32±0.02	37.373	Borucki et al. (2011)	Marcy et al. (2013)
KOI-246.01	5.399	5.97±1.70	2.33±0.02	375.530	Borucki et al. (2011)	Marcy et al. (2013)
KOI-246.02	9.605	2.18±3.50	1.00±0.02	220.199	Borucki et al. (2011)	Marcy et al. (2013)
KOI-261.01	16.238	8.46±3.40	2.67±0.22	73.950	Borucki et al. (2011)	Marcy et al. (2013)
KOI-283.01	16.092	16.13±3.50	2.41±0.20	71.656	Borucki et al. (2011)	Marcy et al. (2013)
KOI-283.02	25.517	8.25±5.90	0.84±0.07	28.891	Borucki et al. (2011)	Marcy et al. (2013)
KOI-292.01	2.587	3.51±1.90	1.48±0.13	851.551	Borucki et al. (2011)	Marcy et al. (2013)
KOI-299.01	1.542	3.55±1.60	1.99±0.22	1581.816	Borucki et al. (2011)	Marcy et al. (2013)
KOI-305.01	4.604	6.15±1.30	1.48±0.08	90.372	Borucki et al. (2011)	Marcy et al. (2013)
KOI-321.01	2.426	6.35±1.40	1.43±0.03	713.204	Borucki et al. (2011)	Marcy et al. (2013)
KOI-321.02	4.623	2.71±1.80	0.85±0.03	291.503	Borucki et al. (2011)	Marcy et al. (2013)
KOI-1442.01	0.669	0.06±1.20	1.07±0.02	3645.770	Borucki et al. (2011)	Marcy et al. (2013)
KOI-1612.01	2.465	0.48±3.20	0.82±0.03	1691.964	Borucki et al. (2011)	Marcy et al. (2013)
KOI-1925.01	68.958	2.69±6.20	1.19±0.03	6.165	Borucki et al. (2011)	Marcy et al. (2013)

<sup>a</sup> Masses, radii, and uncertainties are the literature values.

<sup>b</sup> Planet mass determined by TTVs of a neighboring planet

they should be low, or the converse (RVs that are low when they should be high, and high when they should be low). Because RVs from stellar activity that phase with the expected planet signal will result in an overestimate of planet mass, we must also include the RVs that are anti-phased with the expected planet signal. When Marcy et al. (2013) phase the RV measurements to the transit-determined planet ephemeris, they allow a negative semi-amplitude in the Keplerian fit to the RVs that results in a “negative” planet mass determination. Classically, these planets are considered non-detections, but we include them in the mass-radius relation to avoid statistical bias toward large planet masses at a given radius. Since there is no bias toward large or small planet masses in our sample, we can take the weighted mean mass of planets of a given radius and get a value representative of the planet population.

## 2.2. Inclusion of TTV-discovered planets

Planets discovered by the TTVs they induce on neighboring planets are shown in Figure 3 as orange points. They are systematically less massive than the RV-discovered planets of the same radii. Considering our care to include RV non-detections (i.e. low masses) at all radii in this sample, we cannot attribute this systematic difference between the TTV and RV masses to a bias in the RVs. Either the TTVs are systematically underestimating planet masses (possibly because other planets in the system damp the TTVs), or compact systems amenable to detection through TTVs have lower-density planets than non-compact systems. Detailed comparisons of RV versus TTV masses in a variety of systems will distinguish between these possibilities.

## 2.3. Adopted Errors

We impose a floor of 10% in the planet mass uncertainty, and 5% in the planet radius uncertainty, to compensate in cases where errors might have been underestimated. This is in part because stellar masses and radii, which contribute to the uncertainties in planet masses and radii, are typically known to 10% and 5%, respectively. Also, a conservative estimate of the errors allows us to ascertain whether the scatter about the mass-radius relationship is due to compositional variation among the exoplanets.

## 3. THE MASS-RADIUS RELATION FOR 60 SMALL EXOPLANETS

On average, exoplanet mass increases with increasing radius, indicating an underlying correlation in the individual exoplanet masses and radii. In Figure 3, we show the weighted mean exoplanet mass in bins of width  $0.5 R_{\oplus}$  to highlight the correlation between planet mass and radius.

We calculate the probability that mass and radius are uncorrelated for planets smaller than  $4R_{\oplus}$ . We calculate the correlation coefficient (Pearson R test)  $r = 0.61$ . In our sample of 60 exoplanets, the probability that these data are uncorrelated given  $r = 0.61$  is  $2 \times 10^{-7}$ . Thus, the masses and radii of planets between the sizes of Earth and Neptune are correlated.

To illustrate how this population of exoplanets compares to our Solar System, we indicate the Solar System

planets in Figure 3. A quadratic fit to the exoplanet population happens to line up with the Solar System planets (Lissauer et al. 2011), but has a reduced  $\chi^2$  that is twice as large as the linear fit to the exoplanets. Since most of the exoplanets in this sample have  $P < 50$  days, we do not expect them to behave the same way as Uranus and Neptune, which have orbital periods of tens of thousands of days. Therefore, the hefty masses of Uranus and Neptune compared to planets of similar size that are closer to their stars is not unreasonable.

We present several functional forms to describe the empirical relation between planet mass and radius. Figure 3 shows that planets achieve an Earth-density at about  $1.5 R_{\oplus}$ . If planets smaller than  $1.5R_{\oplus}$  are rocky, they might be better described with a different functional form. We consider separate power-law fits for planets satisfying  $R_P < 1.5R_{\oplus}$  to determine if parameters consistent with rocky compositions better describe those planets.

### 3.1. The Mass-Radius Relation for $R_P < 4R_{\oplus}$

#### 3.1.1. A Linear Mass-Radius Relation

The weighted linear fit to the data for  $R_P < 4R_{\oplus}$  is:

$$M_P/M_{\oplus} = -0.7 + 3.0 R_P/R_{\oplus} \quad (1)$$

with reduced  $\chi^2 = 2.2$  and  $\text{RMS} = 3.8M_{\oplus}$ . The standard errors for the weighted linear fit are  $\text{slope} = 3.0 \pm 0.6$ ,  $\text{intercept} = -0.7 \pm 1.2$ .

#### 3.1.2. A Power-Law Mass-Radius Relation

The power-law fit to the masses and radii for  $R_P < 4R_{\oplus}$  is:

$$\frac{M_P}{M_{\oplus}} = 2.6 \left( \frac{R_P}{R_{\oplus}} \right)^{1.1} \quad (2)$$

with reduced  $\chi^2 = 2.2$  and  $\text{RMS} = 3.8 M_{\oplus}$ . As evidenced by their comparable  $\chi^2$  and RMS, the power law solution and the weighted linear fit describe the masses and radii equally well with equally few parameters, and therefore either is an appropriate description of the data.

### 3.2. The Density Radius Relation for $R_P < 4R_{\oplus}$

#### 3.2.1. A Polynomial Density-Radius Relation

A weighted polynomial fit to the densities and radii for  $R_P < 4R_{\oplus}$  gives:

$$\rho_P = 10.3 - 5.0 \frac{R_P}{R_{\oplus}} + 0.65 \left( \frac{R_P}{R_{\oplus}} \right)^2 \text{ g cm}^{-3} \quad (3)$$

with reduced  $\chi^2 = 1.6$ , and  $\text{RMS} = 61 \text{ g cm}^{-3}$  due to very large uncertainties in density below  $1 R_{\oplus}$  and one outlier. For  $R_P > 1.5R_{\oplus}$ , the RMS is  $2.6 \text{ g cm}^{-3}$ .

#### 3.2.2. A Power-Law Density-Radius Relation

A power-law fit to the densities and radii for  $R_P < 4R_{\oplus}$  gives:

$$\rho_P = 11.7 \left( \frac{R_P}{R_{\oplus}} \right)^{-1.8} \text{ g cm}^{-3} \quad (4)$$

with reduced  $\chi^2 = 1.4$  and  $\text{RMS} = 61 \text{ g cm}^{-3}$  due to very large uncertainties in density below  $1 R_{\oplus}$  and one outlier. For  $R_P > 1.5R_{\oplus}$ , the RMS is  $2.6 \text{ g cm}^{-3}$ . Their similar  $\chi^2$  statistic and RMS make the polynomial and power

law solutions for  $\rho_P(R_P)$  equally good descriptors of the data, but the polynomial solution has the nice analytic property of a finite density at small radii that is only slightly denser than uncompressed iron ( $8.3 \text{ g cm}^{-3}$ ).

### 3.3. A Power-Law Fit to Terrestrial Planets ( $R_P < 1.5R_\oplus$ )

To allow for the possibility of a different relationship between the masses and radii of terrestrial planets, for which we expect rocky compositions with low compressibility, we did an independent analysis of the mass-radius relation for planets smaller than 1.5 Earth radii. The best power-law fit to terrestrial exoplanets is:

$$\frac{M_P}{M_\oplus} = 0.9 \left( \frac{R_P}{R_\oplus} \right)^{4.1} \quad (5)$$

with reduced  $\chi^2 = 0.88$  and  $\text{RMS} = 3.5M_\oplus$ . For comparison, we can apply the power law fit in equation 2 to the terrestrial planets, obtaining reduced  $\chi^2 = 1.7$  and  $\text{RMS} = 2.9M_\oplus$ . The higher power law index results in a slightly smaller  $\chi^2$  statistic, but a slightly larger RMS. Because the uncertainties in density are so large for  $R_P < 1.5R_\oplus$ , we cannot empirically distinguish between these two power law fits to the terrestrial exoplanets. However, our knowledge of physics tells us that for rocky planets that are slightly compressible, we expect  $M_P \propto R_P^{3+\alpha}$ , where  $\alpha > 0$ . Therefore, from a theoretical standpoint, we prefer equation 5 over equation 2 for  $R_P < 1.5R_\oplus$ .

Because the equation of state for rocky planets should not depend on the orbital period of the planet or incident flux on the planet, we can include the terrestrial Solar system planets (Mercury, Venus, Earth, Mars) in a power law fit to the terrestrial planets. We impose uncertainties of 10% in their masses and 5% in their radii so that the Solar system planets will contribute to, but not dominate, the fit to the terrestrial planets. The best power-law fit for exoplanets and Solar system planets with  $R_P < 1.5R_\oplus$  is:

$$\frac{M_P}{M_\oplus} = 1.1 \left( \frac{R_P}{R_\oplus} \right)^{3.4} \quad (6)$$

The reduced  $\chi^2 = 1.3$ , and the  $\text{RMS} = 3.1 M_\oplus$ . The similarity in coefficients between equations 5 and 6 demonstrates that the Solar system planets are not dominating the fit or significantly changing the result. After adding the solar system planets, the  $\chi^2$  minimization favors the higher power law index of equation 6 over the shallower relation for the sub-Neptunes described in equation 2 (reduced  $\chi^2 = 1652$ ).

The different mass-radius and density-radius relations are summarized in Table 1.

## 4. DISCUSSION

### 4.1. Interpretation of the Mass-Radius Relation

The correlation between exoplanet mass and radius for  $R_P < 4R_\oplus$  indicates that Earth-size planets are less massive than Neptune-size planets. Figure 3 demonstrates that planet density decreases as planet mass and radius increase. This can be attributed to an increasing fraction of volatiles with increasing planet size.

Previous works, including Lissauer et al. (2011) and Weiss et al. (2013), suggest that the mass-radius relation is more like  $M_P \propto R_P^2$  for small exoplanets. However, these studies include Saturn or Saturn-like planets at the high-mass end of their populations. Such planets are better described as part of the giant planet population and are not useful in determining an empirical mass-radius relation for small exoplanets. Excluding Saturn-like planets gives a linear (or near-linear) mass-radius relation for small planets.

The moderate reduced  $\chi^2$  values for the linear and power law mass-radius relations ( $\chi^2 = 2.2$ ) presented here indicate that these relations are insufficient to explain the variation in planet mass at a given radius, even after we have imposed conservative estimates on the mass uncertainties. A diversity of planet compositions is required to explain the large scatter in planet mass.

Although most of the planets smaller than  $1.5 R_\oplus$  do not have mass detections better than  $2\sigma$ , their ensemble provides weak constraints on the expected mass of planets smaller than Earth. For instance, none of the planets smaller than Earth has a mass larger than  $10M_\oplus$ , and most have  $M_P < 5M_\oplus$ . Additionally, detections of Kepler-78 b and Kepler-10 b provide significant mass measurements that contribute strongly to a statistical analysis. However, the dearth of data below  $1.5 R_\oplus$  makes it impossible to distinguish between a superior mass-radius relationship in this regime.

In a study of planets with  $M_P < 20M_\oplus$ , Wu & Lithwick (2013) find  $M_P/M_\oplus = 3R_P/R_\oplus$  in a sample of 22 pairs of planets that exhibit strong anti-correlated transit timing variations (TTVs) in the Kepler data. Our independent assessment of 60 exoplanets, 49 of which are not analyzed in Wu & Lithwick (2013), is consistent with this result. Wu & Lithwick (2013) note that a linear relation between planet mass and radius is dimensionally consistent with a constant escape velocity from the planet (i.e.  $v_{\text{esc}}^2 \sim M_P/R_P$ ). The linear mass-radius relation might result from photo-evaporation of the atmospheres of small planets near their stars.

### 4.2. Absence of Correlations to Planet Mass Residuals

We investigate how the residual mass to the mass-radius relationship correlates with various orbital properties and physical properties of the star. To calculate the residual mass, we adopt equation 2 as the nominal mass-radius relationship, and the residual mass is the measured minus predicted planet mass at a given planet radius. The quantities we correlate against are: planet orbital period, planet semi-major axis, the incident flux from the star on the planet, stellar mass, stellar radius, stellar surface gravity, stellar metallicity, stellar age, and stellar velocity times the sine of the stellar spin axis inclination. In these data, the residual mass does not correlate with any of these properties.

#### 4.2.1. A Weak Correlation between Residual Planet Mass and Stellar Metallicity

The stellar metallicities of the stars in our sample are determined by spectroscopy and/or asteroseismology, yielding values accurate to 0.1 dex. We find possible evidence of a correlation between residual planet mass and stellar metallicity for planets smaller than  $4R_\oplus$ . The

**Table 2**  
Empirical Mass-Radius and Density-Radius Relations

Planets	Equation	Reduced $\chi^2$	RMS
$R_P < 4R_\oplus$	$\frac{M_P}{M_\oplus} = -0.7 + 3.0 \frac{R_P}{R_\oplus}$	2.2	$3.8 M_\oplus$
$R_P < 4R_\oplus$	$\frac{M_P}{M_\oplus} = 2.6 \left( \frac{R_P}{R_\oplus} \right)^{1.1}$	2.2	$3.8 M_\oplus$
$R_P < 4R_\oplus$	$\rho_P = 10.3 - 5.0 \frac{R_P}{R_\oplus} + 0.65 \left( \frac{R_P}{R_\oplus} \right)^2 \text{ g cm}^{-3}$	1.6	$2.6^a \text{ g cm}^{-3}$
$R_P < 4R_\oplus$	$\rho_P = 11.7 \left( \frac{R_P}{R_\oplus} \right)^{-1.8} \text{ g cm}^{-3}$	1.4	$2.6^a \text{ g cm}^{-3}$
$R_P < 1.5R_\oplus$	$\frac{M_P}{M_\oplus} = 0.9 \left( \frac{R_P}{R_\oplus} \right)^{4.1}$	0.88	$3.5 M_\oplus$
$^b R_P < 1.5R_\oplus$	$\frac{M_P}{M_\oplus} = 1.1 \left( \frac{R_P}{R_\oplus} \right)^{3.4}$	1.3	$3.1 M_\oplus$

<sup>a</sup> For  $R_P > 1.5R_\oplus$ .

<sup>b</sup> Including terrestrial Solar system planets Mercury, Venus, Earth, and Mars.

Pearson R-value of the correlation is 0.22, resulting in a probability of 10% that the residual planet mass and stellar metallicity are not correlated, given the residual masses and metallicities. However, given that we looked for correlations among 9 pairs of variables, the probability of finding a 90% confidence correlation in any of the 9 trials due to random fluctuation is  $1 - 0.90^9 = 0.61$ , meaning there is only a 39% chance that the weak metallicity correlation is due to an underlying correlation. More measurements of the masses of small planets and the metallicities of their host stars will elucidate whether this correlation is real or the chance arrangement of data.

Buchhave et al. (2012) note that planets smaller than  $4R_\oplus$  form around stars with a large range of metallicities. Their study includes 226 Kepler exoplanet candidates smaller than  $4R_\oplus$ , for which they obtained spectroscopic measurements of  $[m/H]$  in the host stars. Our work uses  $[Fe/H]$  as a metallicity indicator, and we are only considering validated exoplanets. Although Buchhave et al. (2012) find no relation between exoplanet occurrence and host star metallicity for  $R_P < 4R_\oplus$ , they do not comment on the relation between exoplanet size and host star metallicity for small planets. Therefore, a correlation between residual planet mass and stellar metallicity for  $R_P < 4R_\oplus$  would not contradict their result.

## 5. CONCLUSIONS

For exoplanets with  $R_P < 4R_\oplus$  and  $P < 100$  days, planet radius correlates with planet mass with approximately linear scaling, indicating that larger planets have substantially more volatiles than smaller planets. Uranus and Neptune are more massive than the exoplanets of their size in this sample, and they are also at much larger orbital distances than any of the exoplanets in our sample. A study of exoplanets of 3-4  $R_\oplus$  with orbital periods of dozens of years would better contextualize the mass and radius of Uranus and Neptune.

1.5  $R_\oplus$  represents a transition in exoplanet composition: planets smaller than  $1.5R_\oplus$  are denser than Earth and likely rocky, whereas exoplanets larger than  $1.5R_\oplus$  are less dense than Earth and likely contain a substantial fraction (by volume) of volatiles.

Planets satisfying  $R_P < 1.5R_\oplus$  typically have higher densities than Earth, and therefore are likely terrestrial. A power law of  $M_P/M_\oplus = 1.1 (R_P/R_\oplus)^{3.4}$  describes

these planets marginally better than the linear scaling that describes sub-Neptunian exoplanets. However, including the Solar system planets and the theoretical consideration that rocky planets should increase in density as they grow due to compression both favor the higher power law index. More mass measurements of planets like Kepler-78 b and Kepler-10 b are necessary to elucidate an empirical mass-radius relationship for terrestrial planets.

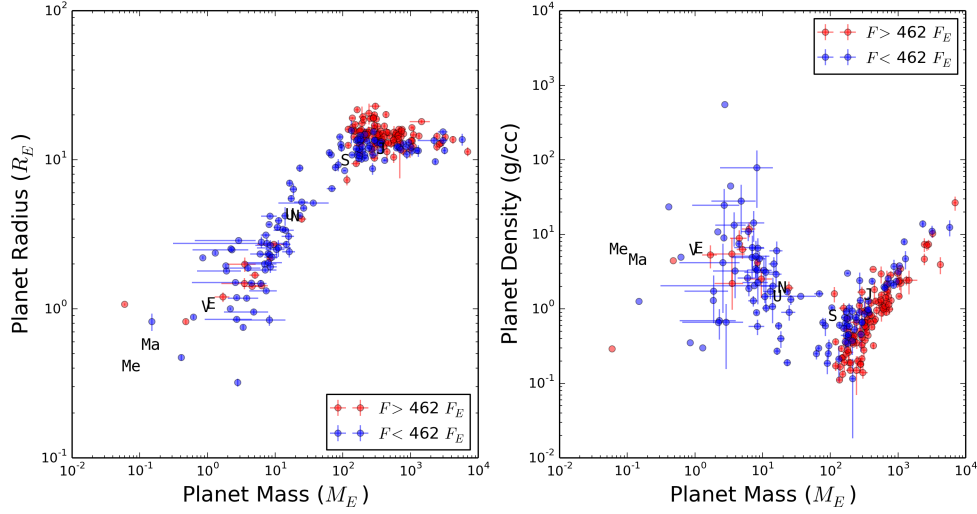


**Figure 1. Left:** Radius vs. mass for 247 exoplanets with measured masses and radii. Below  $150M_{\oplus}$ , planet radius increases with planet mass; above  $150M_{\oplus}$ , planet radius slightly decreases with planet mass. The solar system planets are shown as black triangles for comparison. Planets receiving lower than the median incident flux in this sample (462 times the incident flux at Earth) are blue; those receiving higher than the median incident flux are red. For giant planets (above about  $150M_{\oplus}$ ), planet radius increases with increasing incident flux, whereas for the smaller planets, the relation between radius and incident flux is uncertain. **Right:** Density vs. mass for 243 exoplanets with measured masses and radii. The break at  $150M_{\oplus}$  separates the low-mass planets, for which density decreases with increasing mass, from the high-mass planets, for which density increases with increasing mass. The flux coloration is the same as the left figure.

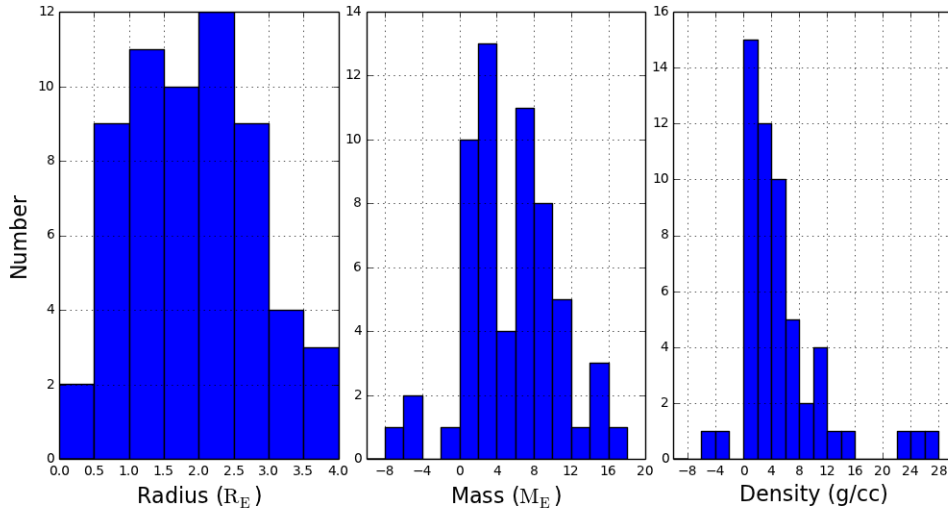


**Figure 2.** Histograms of exoplanet radii, masses, and densities for 60 exoplanets smaller than 4 Earth radii.

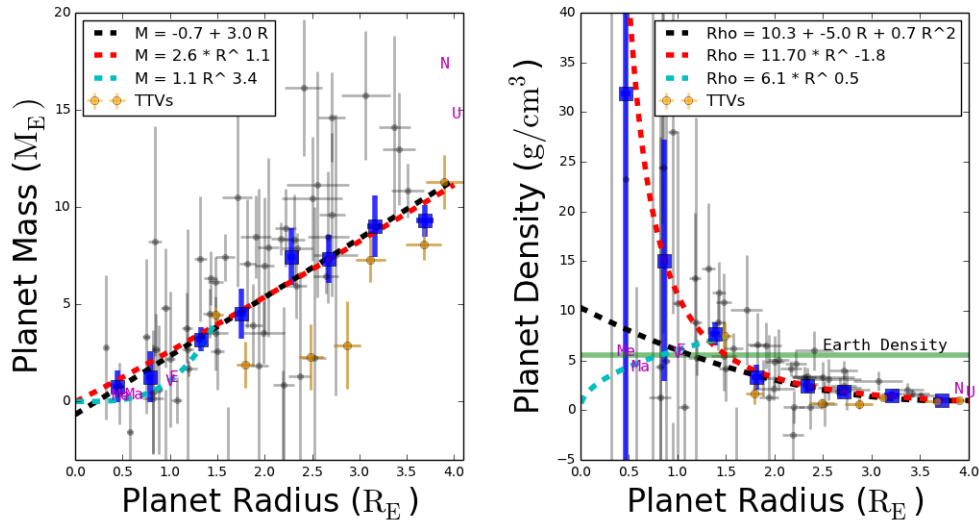


**Figure 3. Left:** Mass vs. radius for 60 exoplanets and  $1\sigma$  error bars (errors were not allowed to go below 10% of the mass or 5% of the radius). Gray points have RV-determined masses; orange points have TTV-determined masses. The dashed lines correspond to the various empirical fits between planet mass and radius; see equations 1, 2, and 6. The blue points are the weighted mean exoplanet mass in bins of  $0.5R_\oplus$ , with error bars representing the uncertainty in the means. The magenta letters indicate solar system planets. The weighted means are to guide the eye only; they were not used in calculating the fits. **Right:** Density vs. radius for 60 exoplanets and  $1\sigma$  error bars (error floors in mass and radius were propagated to density). Gray points have RV-determined masses; orange points have TTV-determined masses. Note that no exoplanets smaller than  $1R_\oplus$  have densities determined to better than  $6.5 \text{ g cm}^{-3}$ . The dashed lines correspond to various empirical fits between planet density and radius; see equations 3 and 4. The blue points are the weighted mean densities in bins of  $0.5R_\oplus$ ; these points are to guide the eye only and were not used in any of the fits. Earth's density is shown as the solid green line. All of the solutions for  $\rho(R_P)$  predict that planets larger than  $1.5 R_\oplus$  will be less dense than Earth, indicating that planets satisfying  $R_P > 1.5R_\oplus$  probably contain a significant fraction of volatiles by volume. Some mass (and density) outliers were excluded from these plots, but are included in the fits.

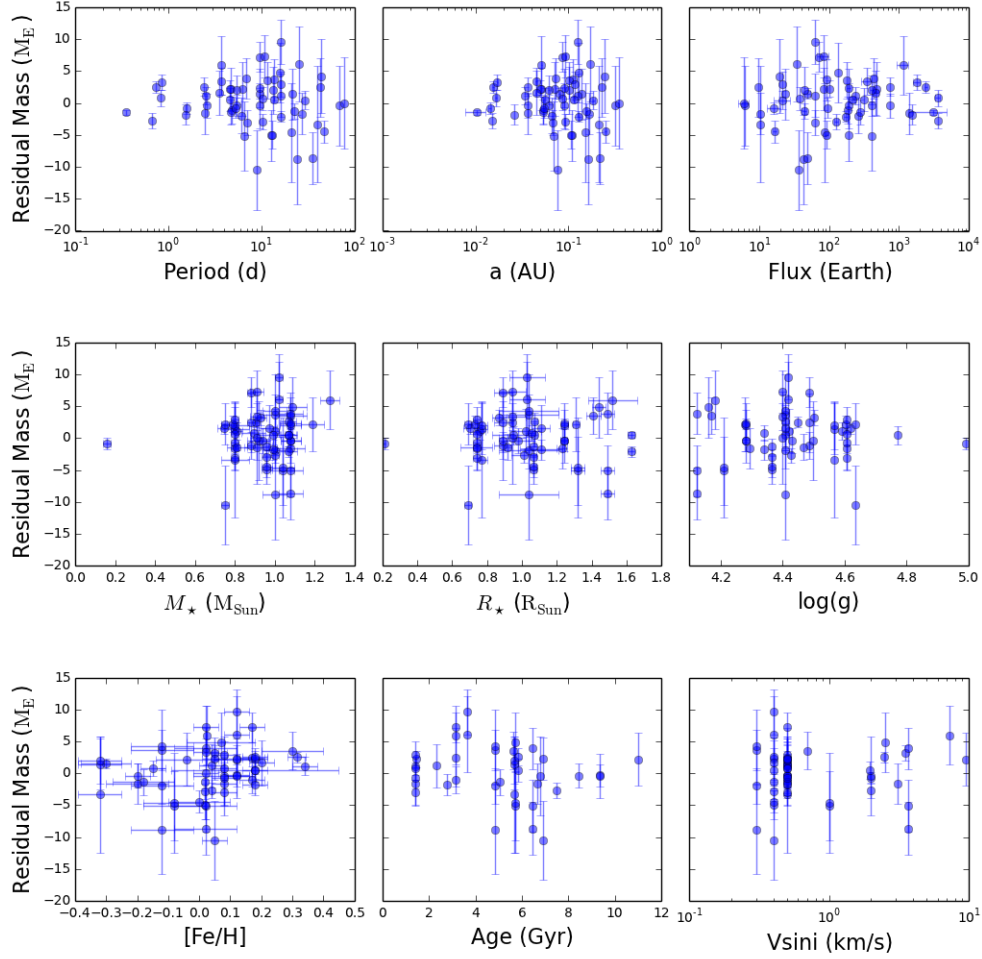


**Figure 4.** Mass residuals (measured minus predicted mass) versus (top left to bottom right): planet orbital period, planet semi-major axis, incident flux from the star on the planet, stellar mass, stellar radius, log surface gravity, log iron fraction (compared to solar), stellar age, and stellar velocity times the sine of the projected stellar inclination. Error bars are  $1\sigma$  uncertainties in mass measurements. None of the residuals show a significant correlation.



## REFERENCES

- Batalha, N. M., Borucki, W. J., Bryson, S. T., et al. 2011, *ApJ*, 729, 27
- Batalha, N. M., Rowe, J. F., Bryson, S. T., et al. 2013, *ApJS*, 204, 24
- Borucki, W. J., Koch, D. G., Basri, G., et al. 2011, *ApJ*, 736, 19
- Buchhave, L. A., Latham, D. W., Johansen, A., et al. 2012, *Nature*, 486, 375
- Carter, J. A., Winn, J. N., Holman, M. J., et al. 2011, *ApJ*, 730, 82
- Carter, J. A., Agol, E., Chaplin, W. J., et al. 2012, *Science*, 337, 556
- Charbonneau, D., Berta, Z. K., Irwin, J., et al. 2009, *Nature*, 462, 891
- Cochran, W. D., Fabrycky, D. C., Torres, G., et al. 2011, *ApJS*, 197, 7
- Dragomir, D., Matthews, J. M., Eastman, J. D., et al. 2013, *ApJ*, 772, L2
- Endl, M., Robertson, P., Cochran, W. D., et al. 2012, *ApJ*, 759, 19
- Enoch, B., Collier Cameron, A., & Horne, K. 2012, *A&A*, 540, A99
- Gautier, III, T. N., Charbonneau, D., Rowe, J. F., et al. 2012, *ApJ*, 749, 15
- Gilliland, R. L., Marcy, G. W., Rowe, J. F., et al. 2013, *ApJ*, 766, 40
- Hatzes, A. P., Fridlund, M., Nachmani, G., et al. 2011, *ApJ*, 743, 75
- Howard, A. W., Johnson, J. A., Marcy, G. W., et al. 2011, *The Astrophysical Journal*, 726, 73
- Howard, A. W., Sanchis-Ojeda, R., Marcy, G. W., et al. 2013, *Nature*
- Kane, S. R., & Gelino, D. M. 2012, *PASP*, 124, 323
- Léger, A., Rouan, D., Schneider, J., et al. 2009, *A&A*, 506, 287
- Lissauer, J. J., Fabrycky, D. C., Ford, E. B., et al. 2011, *Nature*, 470, 53
- Lissauer, J. J., Jontof-Hutter, D., Rowe, J. F., et al. 2013, *ApJ*, 770, 131
- Marcy, G. W., Isaacson, H., & Rowe, J. F. 2013, in prep.
- McArthur, B. E., Endl, M., Cochran, W. D., et al. 2004, *ApJ*, 614, L81
- Petigura, E. A., Marcy, G. W., & Howard, A. W. 2013, *ApJ*, 770, 69
- Queloz, D., Bouchy, F., Moutou, C., et al. 2009, *A&A*, 506, 303
- Sanchis-Ojeda, R., Rappaport, S., Winn, J. N., et al. 2013, *ApJ*, 774, 54
- Sanchis-Ojeda, R., Fabrycky, D. C., Winn, J. N., et al. 2012, *Nature*, 487, 449
- Seager, S., Kuchner, M., Hier-Majumder, C. A., & Militzer, B. 2007, *ApJ*, 669, 1279
- Weiss, L. M., Marcy, G. W., Rowe, J. F., et al. 2013, *ApJ*, 768, 14
- Wu, Y., & Lithwick, Y. 2013, *ApJ*, 772, 74